

Research Article

Fluorescence Intensity and Intermittency as Tools for Following Dopamine Bioconjugate Processing in Living Cells

Rafael Khatchadourian,¹ Alexia Bachir,² Samuel J. Clarke,¹ Colin D. Heyes,³
Paul W. Wiseman,^{2,3} and Jay L. Nadeau¹

¹Department of Biomedical Engineering, McGill University, 3775 Rue University, 316 Lyman Duff Medical Building, Montréal, Canada QC H3A 2B4

²Department of Chemistry, McGill University, 801 Sherbrooke Street West, Montréal, Canada QC H3A 2K6

³Department of Physics, McGill University, 3600 Rue University, Montréal, Canada QC H3A 2T8

Correspondence should be addressed to Jay L. Nadeau, jay.nadeau@mcgill.ca

Received 10 April 2007; Revised 11 August 2007; Accepted 24 December 2007

Recommended by Marek Osinski

CdSe/ZnS quantum dots (QDs) conjugated to biomolecules that quench their fluorescence, particularly dopamine, have particular spectral properties that allow determination of the number of conjugates per particle, namely, photoenhancement and photobleaching. In this work, we quantify these properties on a single-particle and ensemble basis in order to evaluate their usefulness as a tool for indicating QD uptake, breakdown, and processing in living cells. This creates a general framework for the use of fluorescence quenching and intermittency to better understand nanoparticle-cell interactions.

Copyright © 2007 Rafael Khatchadourian et al. This is an open access article distributed under the Creative Commons Attribution License, which permits unrestricted use, distribution, and reproduction in any medium, provided the original work is properly cited.

1. INTRODUCTION

The interactions of semiconductor quantum dots (QDs) with living cells remain poorly understood. QDs of different materials (e.g., CdSe and CdTe), sizes, colors, and surface coatings demonstrate very different toxic effects to cells in culture [1, 2]. Much of the toxicity differences associated with a given type of nanoparticle are attributable to whether the particles are able to enter the cell, escape from endosomes, and enter the nucleus or mitochondria. No satisfactory explanation exists for differences in these properties among batches of particles although there appear to be loose correlations with particle size, particularly for nuclear entry [3]. However, these experiments were performed using thiol-capped particles, and because the small size correlates with thiol coating stability [4], no firm conclusions can be drawn from the results.

A quantitative understanding of the fate of conjugated QDs in biological systems is therefore critical if these particles are to be used in *in vitro* diagnostics or *in vivo* systems. Our previous work demonstrated that QD-dopamine conjugates (see Figure 1) can be used not only as static fluorescent labels, but also as sensors for intracellular redox processes such as endocytosis, lysosomal processing, and mitochon-

drial depolarization [5]. This is due to the electron-donating properties of dopamine (DA), which permit this molecule to act as an electron shuttle between the nanoparticle and other molecules.

The goal of this work is to improve the spatial and temporal resolution of the QD-dopamine redox sensor by determining, in as quantitative a fashion, the relationship between the number of dopamine molecules on the particle and two optical properties which can be measured within the cell: photoenhancement and photobleaching.

The eventual goal is to make an intracellular redox sensor that can yield nanometer spatial resolution. The possibility of several-nanometer resolution would become a reality if the photophysical properties of *single* QDs could be regulated by their immediate environment in a controllable fashion [6]. Fluorescence intermittency, or blinking, is a classic example of a poorly-understood feature of QD fluorescence that is often neglected or suppressed rather than exploited. Under continuous illumination, single QDs exhibit blinking over a wide range of timescales [7–12]. A number of studies have been reported which look at various effects on blinking, such as excitation power [8, 9, 11, 13, 14], the shell material around the QDs [7, 8, 10], as well as environmental conditions such as temperature [8, 15] and surrounding

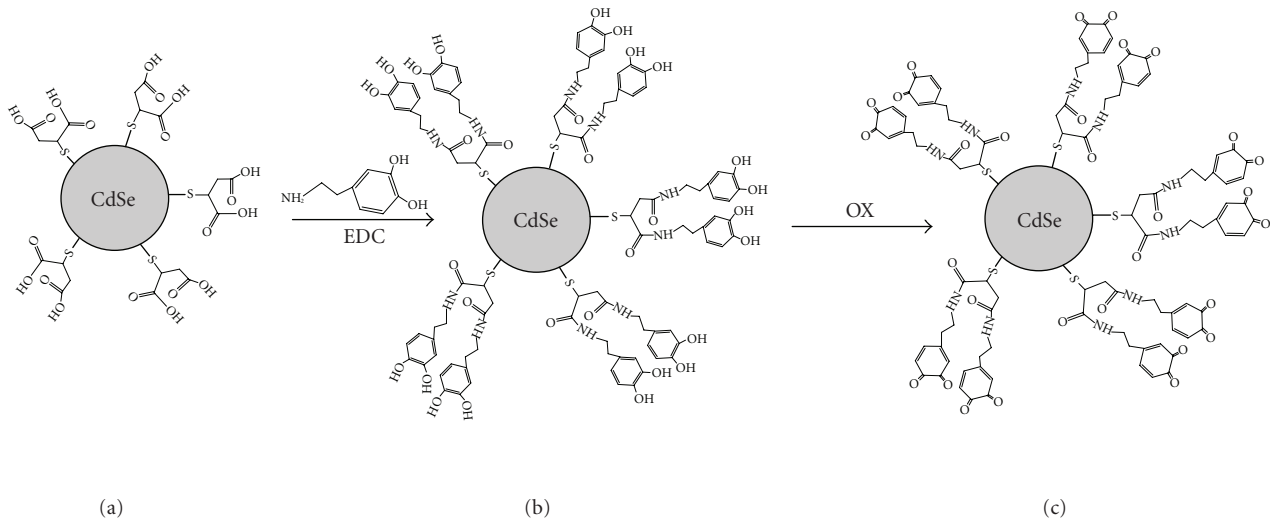


FIGURE 1: Schematic of QD-dopamine conjugate preparation and mechanism of redox sensitivity. (a) MSA-capped QD. (b) Upon addition of dopamine (structure shown above arrow) and the zero-length cross-linker EDC, an amide bond is formed between the amine of dopamine and the carboxylate groups of MSA. This schematic shows 100% linkage of dopamine to MSA termini; however, we show here that this ratio can be controlled. (c) Upon oxidation ("OX"), the catechol becomes a less-soluble quinone.

medium [16, 17]. From these studies, two physical models have been advanced which attempt to explain the inverse power law behavior of the blinking statistics. The first model assumes a fluctuating distribution of electron traps in the immediate vicinity of, but external to, the QD [18]. Tunneling of the electron out of the QD results in a charged particle, quenching any emission and, thus, resulting in an off state. Neutralization of the QD by recapture of the electron recovers the emission, resulting in an on state. The second model does not assume external traps, but rather posits internal hole traps, presumably at surface states or crystal imperfection sites [19]. Energetic diffusion of the electronic states results in a time-dependent resonance condition in which Auger-assisted trapping of the hole results in an off state. Given the variability of the possible mechanisms, it is not possible to predict the effects of conjugation of a redox-active molecule such as dopamine. In this work, we evaluate the effects of dopamine of blinking and evaluate the possibility of the use of intermittency as a tool for the ultrasensitive detection of subcellular environments and biochemical processing of QD-bioconjugates.

2. RESULTS

2.1. Quantifying numbers of conjugates per particle

In this study, we used red-emitting CdSe/ZnS QDs (QD605, emission peak 605 ± 20 nm) for photoenhancement and blinking studies, and green-emitting QDs (QD560, emission peak 560 ± 20 nm) for cellular uptake studies. QDs were conjugated to the neurotransmitter dopamine via the primary amine located on the opposite end of the molecule from the redox-active catechol (see Figure 1). The number of bound ligands was quantified in EDC-coupling reactions containing varying concentrations of dopamine and/or of 1-ethyl-3-(3-

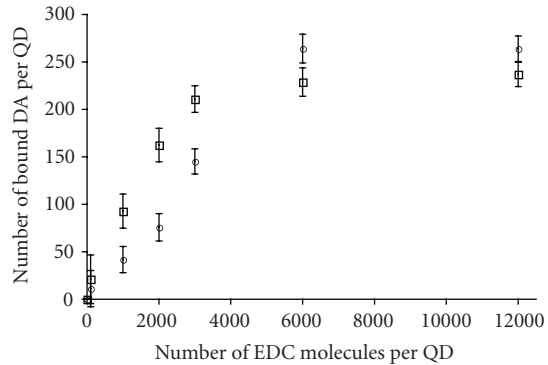


FIGURE 2: Number of bound dopamine molecules as a function of the number of EDC added to the coupling reaction for QD560 (squares) and QD605 (circles) as measured by OPA assay. Data are an average of three experiments with error bars indicating the standard error of the mean.

dimethylaminopropyl) carbodiimide hydrochloride (EDC), using the o-phthaldialdehyde (OPA) assay as described previously [20]. A strong dependence was observed of the number of EDCs per QD on the number of dopamine molecules that bound. The number of bound ligands increased linearly with the number of EDC molecules until a certain breakpoint and a plateau was reached, which was considered as the saturation point for the QDs (see Figure 2). Indirectly, we can interpret the saturation point as an indicator of the number of functional groups available on the surface of the QDs. This appears to be slightly smaller for green QDs than for red, as expected due to the smaller size of these particles, although it is the same within error at the maximum EDC concentration.

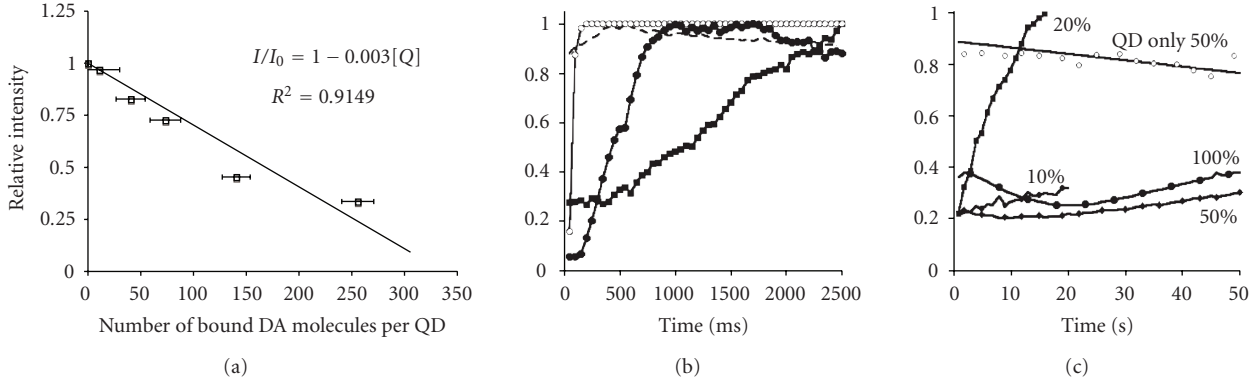


FIGURE 3: Relationship between the number of dopamine molecules bound to the surface of QD605 and the resulting emission intensity. (a) The quenching observed upon conjugation is nearly logarithmic. Data are an average of three experiments with error bars indicating the standard error of the mean. (b) Unquenching of QD-dopamine conjugates with varying amounts of coverage under Hg-lamp exposure (QD filter set, see Methods). Each symbol is a data point, with error bars smaller than symbols ($n = 3$). Bare QDs alone (dashed line) show essentially constant fluorescence over a 2.5-second exposure period; they begin to photobleach near the end. QDs, to which dopamine was added but not conjugated (no EDC) (open circles), achieve maximum fluorescence within 50 milliseconds. Conjugates with 40 ± 14 DA/particle (filled circles) brighten over a time course of ~ 700 milliseconds. The conjugates with the greatest coverage (filled squares, 255 ± 14 DA/particle) have just begun to plateau at 2.5 seconds. (c) Confocal laser illumination of samples with 255 ± 14 DA/particle. Photoenhancement showed a strong dependence upon laser power, with efficient enhancement at 20% but limited or no enhancement at 10%, 50%, and 100% power. Each symbol is a data point, with error bars smaller than symbols ($n = 5$). Unconjugated QDs showed similar bleaching curves for all powers tested (shown: 50%).

2.2. QD-dopamine fluorescence properties

Manipulating the extent of ligand coverage of the QD surface can be an effective way to modulate fluorescent properties if the ligands can act as energy or electron donors or acceptors to or from the QDs. In our previous work, we have shown that dopamine can be used to modulate the emission characteristics of QDs by a mechanism of electron transfer. In Figure 3(a), we demonstrate the effect of the number of bound dopamine ligands and the subsequent reduction in the emission intensity of the QDs. To distinguish this type of quenching from the Stern-Volmer collisional quenching, we purified the conjugates from excess unbound ligand. Our results showed a large decrease in intensity when a relatively small number of ligands were bound to the surface, owing to the electron transfer from dopamine to the QDs [5].

Oxidation of these quenched QDs, either by photoexposure or chemical means, led to a restoration of fluorescence from the QD. In addition, oxidized dopamine emitted fluorescence in the blue regime (peak emission 460 nm). Thus, there were three parameters that could be used to indicate the number of dopamine conjugates on the particle surface: (a) blue fluorescence from oxidized dopamine; (b) brightness of QD fluorescence without UV pre-exposure; and (c) time course of QD fluorescence under photooxidation.

This latter quantity must be determined for each light source; broad Hg-lamp excitation (through a QD or DAPI filter, see Figure 3(b)) yielded very different results than 488 nm laser-line excitation, showing essentially all-or-nothing dependence on illumination power (see Figure 3(c)). Similarly, lifetime measurements with time-correlated single photon counting (TCSPC) and 400 nm

laser illumination revealed extreme sensitivity to illumination power. A full study with laser powers varying from tens of microwatts to several milliwatts is forthcoming.

2.3. Improved spatial resolution of redox sensing in living cells

QD-dopamine was readily endocytosed by cells bearing dopamine receptors. Little or no binding was seen to cells without dopamine receptors, and the QD conjugates were readily washed away [5]. We investigated the effect of dopamine ligand coverage and corresponding uptake in DA-receptor-expressing PC12 cells. As expected, cells that were treated with QDs alone did not show any detectable QD association. For the QD560-DA conjugates, particles with fewer than 100 DA/particle were not taken up in significant amounts after 15–30 minutes of incubation (not shown). Thus, particles that were effectively taken up began with slow photoenhancement curves. The variation of photoenhancement properties with position in the cell was then used to semiquantitatively identify regions where oxidation had occurred.

The location and appearance of various organelles in cells were determined by labeling with specific dyes such as Lysotracker and Mitotracker (see Figure 4). Studies of unquenching time-courses of the simultaneously loaded QD-dopamine were then performed under 488 nm laser illumination. The results showed a consistent and reproducible pattern with three distinctive QD behaviors. In fixed cells, with depolarized mitochondria, QDs did not show overlap with the mitochondrial-targeting dye MitoTracker. QD fluorescence brightened slightly under light exposure

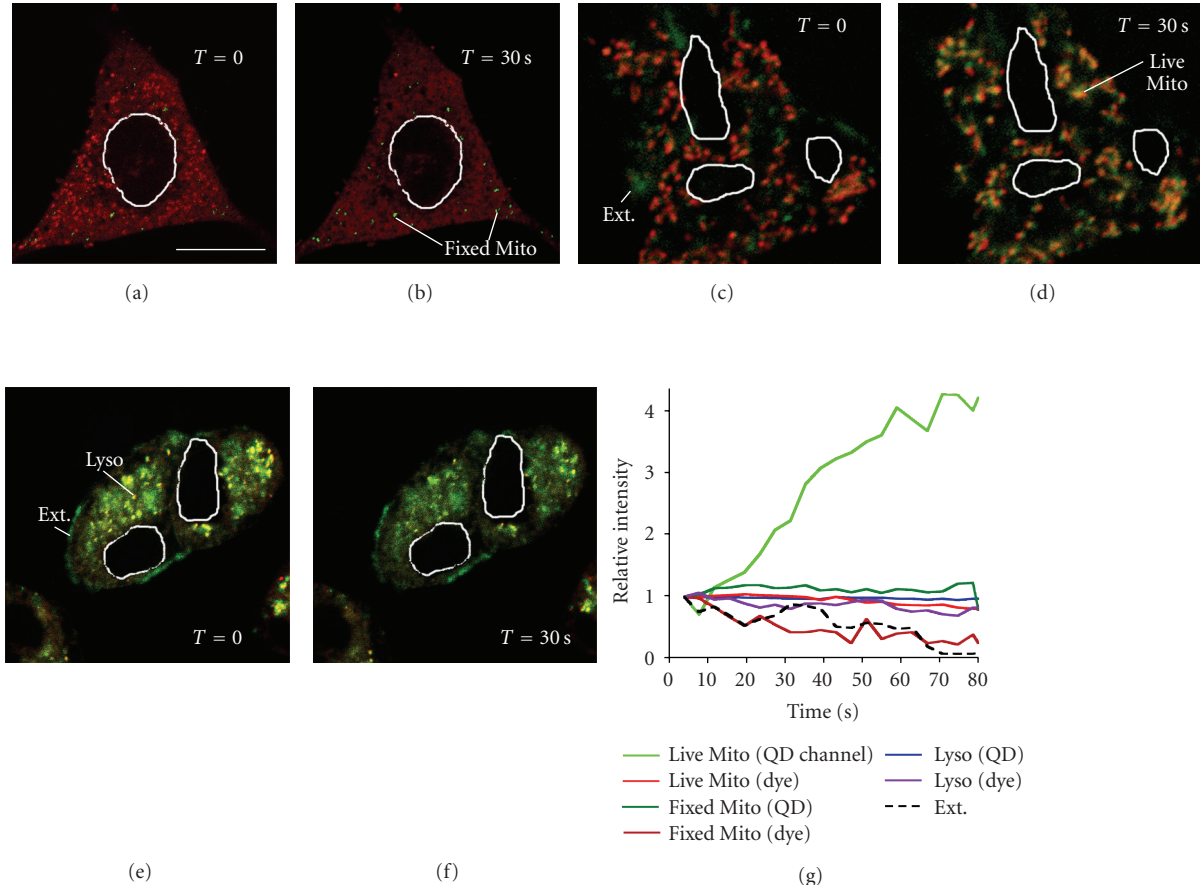


FIGURE 4: Confocal images and time courses of QD-dopamine with 100 ± 10 DA/particle in PC12-dopamine receptor cells colabeled with organelle dyes. Scale bar = $10 \mu\text{m}$ for all panels; in all panels, the green channel indicates the QDs and the red channel the organelle dye. The white lines indicate the cell nuclei. (a) Paraformaldehyde-fixed cell labeled with MitoTracker and QDs. (b) The same cell after 30 seconds of laser-light exposure. (c) Live cells labeled with MitoTracker and QDs. (d) The same cells after 30 seconds of laser-light exposure. (e) Live cell labeled with Lysotracker and QDs. (f) The same cell after 30 seconds of light exposure. (g) Relative intensities from the indicated regions over 100 seconds of exposure time.

(see Figures 4(a), 4(b), and 4(g)). In live cells, however, the mitochondrial region brightened quickly and intensely, with QD-Mitotracker overlap becoming apparent (see Figures 4(c), 4(d), and 4(g)). In both live and fixed cells, a good deal of QD fluorescence was seen colocalized with lysosomes. QD fluorescence within lysosomes shows only bleaching with time (see Figures 4(e), 4(f), and 4(g)). QDs that were outside the cell, in aggregates outside the membrane, exhibited no brightening but only photobleaching over time (see Figures 4(e), 4(f), and 4(g)).

Observation of the blue QD-dopamine fluorescence confirmed what was suggested by the time-course spectra. QDs outside the cells showed no blue emission, confirming the absence of dopamine, whereas those in the cytoplasm and mitochondria showed visible 460 nm emission (see Figure 5).

2.4. Effect of dopamine on fluorescence intermittency

Blinking is conveniently studied by taking an image series with time of a number of immobilized QDs [9–11]. Details

of the analysis may be found in the methods section and in previous publications [9, 10]. The result of the analysis is that the fluorescence time trace for each identified QD is extracted from the image series, and the durations of on and off times (time durations for which the signal is above and below the threshold level, resp.) are extracted. A typical image and extracted fluorescence trace of a single, immobile QD are shown in Figure 6.

We studied the effect of conjugating dopamine to QDs on their blinking statistics. The probability distributions of on times, $P(\text{on})$, and off times, $P(\text{off})$, for QDs with and without conjugated dopamine are shown in Figures 7(a) and 7(b), respectively, as measured by extracting fluorescence time traces, such as shown in Figure 6(b), setting a threshold and calculating on and off times. Approximately 500 QDs were analyzed from 5 sets of movies, taken at 50-millisecond resolution for 100 seconds. Except for the dopamine, the QDs and the experimental conditions were identical. Clearly, under these conditions, the conjugation of dopamine to the QD reduced the on times and increased the off times.

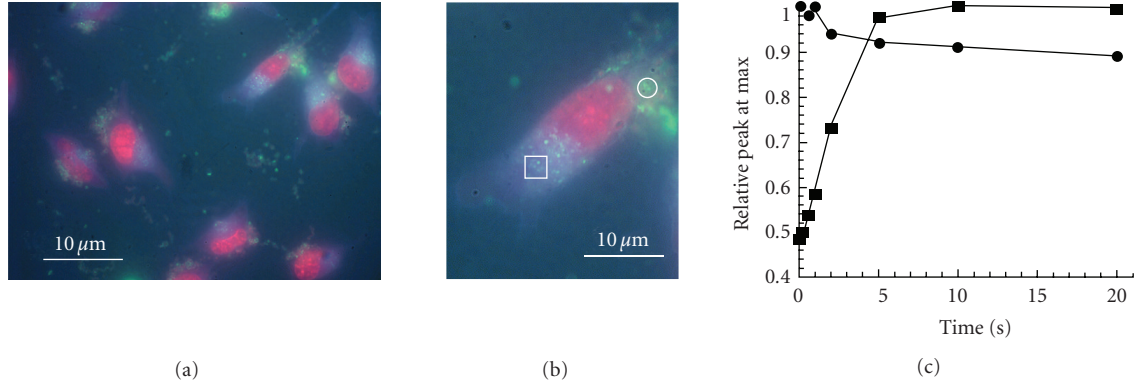


FIGURE 5: Subcellular differences in QD-dopamine fluorescence. (a) Image under DAPI filter of cells labeled with QD-dopamine (and with SYTO red to show nuclei). The green regions (540–580 nm emission) show QD fluorescence but no dopamine fluorescence. The blue areas (460–500 nm emission) show dopamine fluorescence and no initial QD fluorescence; QD fluorescence appears after UV illumination. Double-labeling experiments identified the green areas as lysosomes (not shown) or as regions exterior to the cell. (b) Closeup of a single cell from panel A showing blue spots (square) and green spots (circle). (c) Time course of QD peak fluorescence under UV illumination (QD filter) for a blue region (squares) and a green region (circles).

3. DISCUSSION

3.1. Tracking QD oxidation with fluorescence changes

We previously showed [5] that QD-dopamine conjugates show altered fluorescence in living cells in accordance with the cellular and subcellular redox potential with brighter fluorescence corresponding to more oxidizing conditions. However, two of the observed phenomena were not fully explained. First, different colors, batches of QDs, and conjugate preparations showed widely varying degrees of uptake. Second, the mechanism of brightening in response to oxidation was not elucidated although it was presumed to be related to cap decay [21].

In this work, we explain the differing levels of uptake by showing that using standard MSA-EDC coupling techniques, approximately 100 dopamines per particle are required to obtain efficient uptake in our stably transfected dopamine-receptor cell lines. Future work will explore variations on solubilizing-agent chain length and the addition of spacers [22] to improve the presentation of the dopamine to its receptor, as this high requirement probably reflects biological inactivity of most of the dopamines on these particles.

Of general interest is the observation that controlling the average number of dopamine molecules bound to QDs affects the photoenhancement of ensembles of particles in a measurable fashion. This makes these conjugates a more useful tool than one based upon quenching alone, as the presence of fully-quenched particles can obviously not be detected under fluorescence microscopy. On slides, more dopamines per particle correspond to slower photoenhancement (see Figure 3(b)); QDs without dopamine show bleaching without enhancement.

Confocal laser illumination shows a quite different pattern from Hg-lamp illumination; this could be due to several factors. The illumination is at a single wavelength; the most commonly used line (488 nm) will not excite the dopamine

quinone, eliminating issues of signal confusion as well as eliminating the possibility that excitation of the quinone affects the QD enhancement or bleaching. Finally, laser illumination is intermittent due to scanning, perhaps permitting QDs to recover in-between pulses.

In cells, a minimum number of dopamines, corresponding to slow enhancement, is necessary for uptake. However, as the particles travel through the cell, particularly to oxidizing regions, enhancement becomes more rapid suggesting that the cap decay mechanism is in fact correct. These data could be used for a semiquantitative model of QD processing in cells (Schematic in Figure 8).

3.2. Blinking analysis

It is immediately obvious from Figure 7 that the addition of dopamine to the QD surface affects blinking by reducing on times and increasing off times. Many groups have found that the distribution of off times fits to a power law function [8–10, 12, 18, 23], whereas the on times distribution is the source of some debate. Some have found that the on times fit to a power law function [18, 24]; whereas others have found that they fit better to a power law function convoluted with an exponential function at long on times [8, 10, 19]. The effect of coating the CdSe with a ZnS shell on the blinking has also been studied by several groups. Nirmal et al. found that a thick ZnS shell results in the observation of longer on and off events [7]. Subsequently, a more thorough statistical analysis revealed that the power law slopes for both the on times and the off times distributions are not affected by ZnS capping, but that the exponential cutoff time in the on times slightly increases by ZnS capping [8]. Heyes et al. found that, within experimental error, there was no effect in both the power law slope and the exponential cutoff upon increasing the ZnS capping thickness [10]. This lack of dependence was explained as the physical origin of blinking lying in hole-trap states at the surface or core-shell interface.

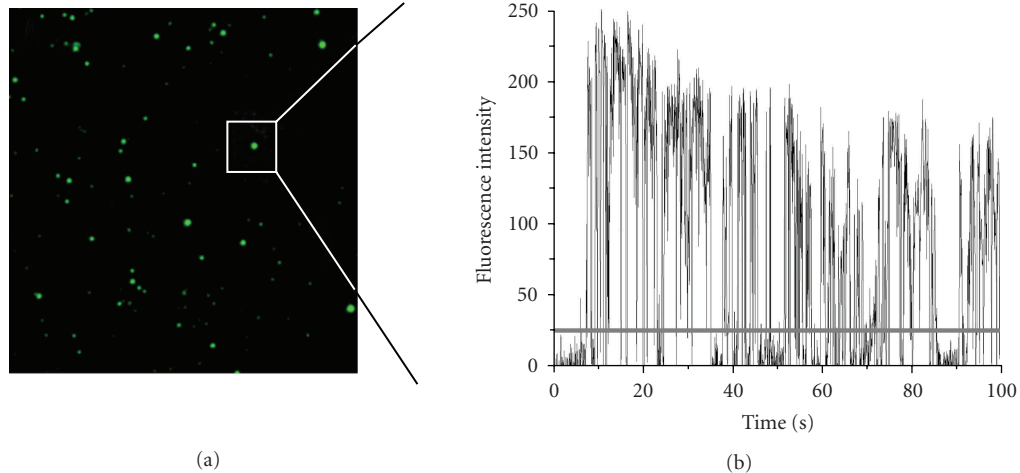


FIGURE 6: Evaluation of QD blinking. (a) Typical image of immobilized QDs. Due to their different brightness, some spots appear larger than others. Single QDs are identified by the size of their point spread function and selected for subsequent analysis. Image size is $40 \times 40 \mu\text{m}^2$. (b) Typical intensity trace of a single QD under continuous excitation. The grey line indicates an arbitrary threshold used to separate on-events from off-events. The threshold is usually set to 2–3 standard deviations above the background noise level, which is determined from nearby pixels containing no QD.

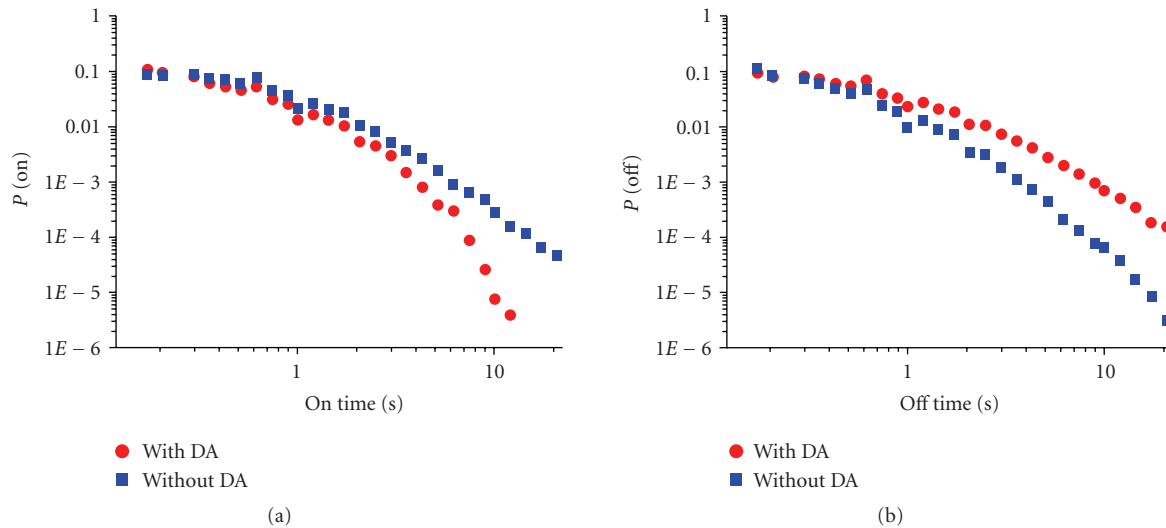


FIGURE 7: Probability histograms for (a) on-times and (a) off-times durations with (red) and without (blue) dopamine conjugated to the QD surface. A strong effect of dopamine in both on-times and off-times durations is evident. The addition of dopamine reduces the probability of observing long on-times and increases the probability of observing long off-times.

In the study of Heyes et al. [10], all blinking probability distributions fit to an inverse power law for off times. For on times, the functions fit to an inverse power law with exponential cutoff at longer on times, in agreement with previous observations and a previously published model, which did not assume the presence of external trap states [19]. The data presented here do not fit to the same functions as previous observations (power law for off times and a power law convoluted with an exponential cutoff at longer times) suggesting that the underlying mechanisms of blinking differ. At

the current time, we cannot identify the source of these differences and much more work is needed to further investigate the physical origins. We have identified several possible sources that may be responsible for the observed difference in blinking statistics. One such source may be that the difference in chemical environment of the QD is responsible. The QDs used here are coated with mercaptosuccinic acid (MSA) ligands, which carry both a negative charge and a coordinating sulfur group which may both affect the blinking statistics. Most previous studies have investigated QDs

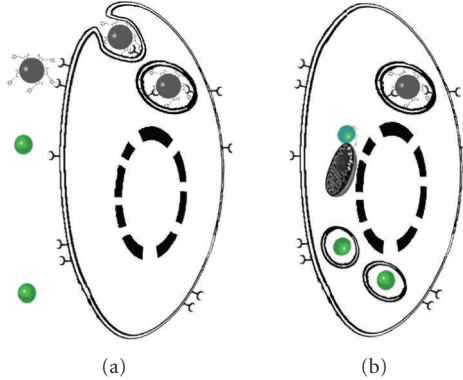


FIGURE 8: Fluorescent tracking of QD uptake and breakdown in cells (cellular structures not to scale). (a) QDs conjugated to an electron donor can bind to specific receptors (gray sphere) but are not immediately fluorescent. QDs that have lost this surface cap are immediately green-fluorescent (green spheres) but do not bind to receptors and are rarely endocytosed. (b) Processing through the cell leads to changes in surface cap and resulting alterations of fluorescence. Areas of normal cellular redox potential such as endosomes (gray) are not fluorescent unless illuminated for significant amounts of time. Highly oxidizing areas such as lysosomes, in contrast, show immediate green fluorescence and no blue fluorescence without photoenhancement, indicating that the conjugate has been removed from the particle, probably due to proteases in the lysosome. Particles near mitochondria show varying degrees of green and blue fluorescence with slow photoenhancement.

that are either coated with uncharged organic ligands or are coated with large amphiphilic polymers. The chemical environment may be further affected by the conjugation of dopamine which may result in the presence of different trap (off) states. Another source for the difference may lie in the fact that in the experiments presented here, polychromatic excitation from a halogen lamp, passed though a QD filter cube, which results in excitation with a range of wavelengths from 380 nm to 460 nm, was used. While this excitation configuration is a common one for biological detection of QDs in cellular environments, both the CdSe core and the ZnS shell are excited (as well as dopamine when it is present) whereas most previous blinking experiments have been performed using monochromatic excitation at either 488 nm, 514 nm, or 532 nm [7–12] where only the CdSe core is excited. Excitations formed following excitation of the QDs using the present excitation configuration are more easily exposed to the QD surface or surrounding environment. Further work is currently underway in our lab to identify the effects of both the ligand properties and the excitation energy on the blinking mechanism.

Bleaching of QDs is also affected by the addition of dopamine. The average intensity of the images decreases faster for QD-dopamine conjugates than for QDs not conjugated with dopamine. However, the decrease in average intensity is relatively small compared to the total intensity due to the contribution from the background signal arising from the many pixels in which no QDs are present. This is constant throughout the experiment, which contributes to a nonzero

offset in the integrated intensity of the image. On the other hand, the fraction of particles in the on state decreases by approximately 3 orders of magnitude for the QD-dopamine conjugates, whereas QDs without dopamine show a relatively constant on fraction during the experiment. This reduction in the fraction of emitting QDs indicates that either they are trapped in a long off time or that they are permanently bleached. Chung and Bawendi argued that there must exist a saturation in the maximum off time duration in order to explain the observation that, under continuous illumination, QD emission does not reach zero intensity due to all QDs eventually becoming trapped in a very long off state [25]. Indeed, using ensemble fluorescence spectroscopy, they determined that the maximum off time is on the order of thousands of seconds—a timescale that is generally not reached using single molecule experiments. In order to determine if the nonfluorescent particles would turn “on” again at later times (i.e., the particles are in an extended off period), we turned off the excitation source for several minutes. We then imaged the same area to determine if the particles were once again fluorescent. We found that almost none of the particles regained their fluorescence, indicating that the photobleaching was indeed permanent rather than the particles residing in an extended off period. It has been shown that QDs are much more photostable than other fluorophores, and are generally photostable for timescales much longer than our experiments. Dopamine itself must be a significant source of the photobleaching. One possible mechanism may be that radicals are formed by the dopamine, which may then eventually diffuse through the solution and react with the QD surface forming trap states. This may repeat until a significant number of trap states are formed which results in preferential nonradiative decay rather than radiative decay of any formed excitons. It must also be noted here that, under these excitation conditions, dopamine is also directly excited. The initial increase in on fraction of QDs may be the result of an initial bleaching of dopamine on the QDs which results in more on particles. This may be then followed by reaction of radicals with the QD to once again turn them off. Further chemical characterization of the bleached particles is necessary to test these hypotheses.

The changes in blinking statistics upon conjugation of QDs to specific ligands such as dopamine suggest that such an assay may be used in the future as ultrasensitive sensors for chemical and biological characterization of subcellular environments and biological processing pathways. However, it is necessary for the underlying mechanisms contributing to the observed changes to be fully understood in order to interpret these types of experimental results.

3.3. Conclusion

Conjugation of QDs to an electron donor such as dopamine leads to changes in optical properties beyond simply quenching. These properties, such as photoenhancement and blinking, may be used in biological studies as novel means to probe subcellular environments. The use of other electron donors, such as any of the biological catechols, should show equally interesting properties when conjugated

to QDs, creating a general principle upon which new fluorescent indicators may be created.

4. METHODS

4.1. QD synthesis

All chemicals were purchased from Sigma-Aldrich Canada (Oakville, ON, Canada). CdSe/ZnS core-shell nanocrystals were synthesized as previously described [26, 27]. In brief, CdSe/ZnS QDs were synthesized as follows: 0.024 g CdO was added to a reaction flask containing 0.44 g stearic acid and heated to 180°C under inert conditions, forming a colorless solution. The solution was allowed to cool, and afterwards 5 g TOPO and 2 g octadecylamine were added to the flask. The flask was then evacuated and filled with inert gas several times, and the solution was heated to 200°C–300°C (exact temperature depends on the desired size). 0.2 g Se was then dissolved in 2–4 mL TOPO under inert conditions, and added to the reaction flask. Finally, 0.4 mL of Zn(Me)₂ was added to 0.07 mL (TMSI)₂ under an inert atmosphere, and added to the reaction flask. Finally the solution was allowed to cool, dissolved in CHCl₃, and precipitated with MeOH. The precipitate was collected by centrifugation and washed several times with MeOH. These TOPO-passivated nanocrystals were then dispersed in the desired solvent, including toluene, CHCl₃, and hexane. QDs were solubilized using MSA. Aqueous QD solutions were diluted in H₂O to an optical density (OD) of 0.1 at the exciton peak. This corresponds to an approximate concentration of 1 μM [26]. All QDs were stored in the dark until ready for use.

4.2. Conjugation to dopamine

One mg EDC was added to 0.2 mL of QDs in aqueous solution and 0.3 mL phosphate-buffered saline (PBS) solution. The tubes were covered in foil and put on a shaker for one hour. Afterwards dopamine was added to a final concentration of 2 mM, and PBS was added to a final volume of 1 mL. The tube was again covered in foil, and agitated on a shaker for 2 hours. Solutions were dialyzed against PBS for 1 hour in order to remove excess dopamine. All handling of dopamine solutions and QD-dopamine was performed in a glove bag under nitrogen to avoid oxidation of dopamine and further stored under an inert atmosphere until ready for use.

4.3. Incubation of QDs with cells

Experiments with cell lines were performed using PC12 cells stably transfected with human D2 dopamine receptors (gift of Stuart Sealfon, Mount Sinai School of Medicine). Cells were maintained in high glucose Dulbecco's Modified Eagle's Medium (DMEM) (Invitrogen Canada, Burlington, ON, Canada) supplemented with 10% fetal bovine serum, 5% horse serum, 0.2 mM glutamine, 100 U/mL penicillin, and 100 μg/mL streptomycin in a 5% CO₂ atmosphere at 37°C. For passage, cells were rinsed first with phosphate-buffered saline (PBS) and then with Hanks balanced salt solution containing 0.05% trypsin and 0.02% EDTA, incu-

bated for 2 minutes at room temperature, and resuspended in supplemented DMEM. Cells were passaged onto glass bottom dishes (MatTek Co., Ashland, Mass, USA) the day before use at 50–80% confluence. Just prior to labeling, growth medium was removed by 2 washes in sterile PBS, and then replaced with 1 mL serum-free medium without phenol red (OptiMem, Invitrogen Canada). In preliminary studies, incubation times were varied between 15 minutes to 2 hours, and it was found that some uptake of unconjugated QDs could occur at longer timescales. Thus, all data presented show cells incubated for 15 minutes. QD-dopamine conjugates were applied directly into serum-free medium at a concentration of ~5–10 nm particles. For co-labeling with MitoTracker Red or Lysotracker Orange (Invitrogen Canada), dyes were added to cells at a concentration of 1 μM at least 30 minutes before QD addition. All cells were washed several times with sterile PBS after labeling, and live cells were imaged in PBS. Fixed cells were incubated in 3.7% paraformaldehyde in PBS for 30 minutes, rinsed twice in PBS, and imaged in PBS.

4.4. Spectroscopy and microscopy of cells

Absorbance and emission spectra were recorded on SpectraMax Plus and SpectraMax Gemini readers (Molecular Devices, Sunnyvale, Calif, USA). For Hg-lamp exposure experiments, cells and QDs were examined and imaged with an Olympus IX-71 inverted microscope and a Nuance multispectral imaging system, which provides spectral data from 420–720 nm in 10-nm steps (CRI Instruments, Cambridge, Mass, USA). The objective lens was a Nikon PlanFluor 100× (N.A. = 1.30). Illumination was through a "QD" filter cube set (excitation = 380–460 nm, dichroic = 475 nm, emission = 500 LP), a "DAPI" filter cube set (excitation = 350/50nm, dichroic = 400 nm, emission = 420 LP), or a "TRITC" filter set (excitation = 540 nm, dichroic = 565 nm, emission 605 LP) (Chroma Technologies, Rockingham, Vt, USA). For evaluation of photoenhancement on slides, a droplet of QD solution was placed on a glass slide and illuminated at full lamp power from below using the QD filter. Data were excluded if the sample dried out during imaging.

Confocal imaging and time-course experiments were performed on a Zeiss 510 LSM with a Plan Apo 100× oil objective. QDs were excited with an Ar ion laser with output power held at 55% for all experiments, corresponding to 6 A of tube current to reduce laser flicker, and the percent transmission of the 488 nm line was adjusted between 10% and 100%. Lysotracker Red and MitoTracker Orange were excited with a HeNe laser (543 nm line). Cells labeled with >1 probe were examined for channel bleed-through before imaging. For cell imaging studies, the 488 nm line was kept at 50% of maximum power.

Samples were prepared for blinking studies by aminosilanizing a glass coverslip with aminopropyl trichlorosilane to which a drop of ~100 pM QD solution was added. QDs were immobilized by electrostatic forces between the positively charged amino groups of the silane and the negatively charged carboxylates on the QD. The QDs were measured with the liquid still above them to reduce possible

effects from oxygen in the atmosphere. Drying out of the solution was reduced by placing a reservoir of water next to the sample, and covering the sample stage, which resulted in a humid environment around the sample. Blinking studies of QDs were performed in an epifluorescence configuration on an Olympus IX70 inverted microscope using a halogen-lamp source. A QD filter cube set was used for excitation and emission (excitation = 380–460 nm, dichroic = 475 nm, emission = 500 LP). The excitation light was passed through an Olympus PlanApo oil-immersion objective (60×, 1.45 NA) and the emission collected into the same objective. The light is then focused onto a Photometrics Cascade 512 B EM-CCD camera, and a time-stack of images taken at 20 fps (50-millisecond exposure) for 2000 frames using the RSImage software (Roper Scientific, Tucson, Ariz, USA). The images are stored in 16-bit TIFF format for subsequent analysis. Homemade software was written by Dr. Andrei Kobitski at the University of Ulm (Germany) using Matlab 6.5 (Mathworks, Natick, Mass, USA), from which traces of individual QDs are extracted and probability distributions of on and off times are determined. The details of the analysis may be found in previous publications [9, 10]. Briefly, the algorithm aligns each frame of the series and integrates the image stack. Thus, QDs that are on at least once in the time series will be identified. Then, the software measures the integrated signal from the 3×3 pixels around the central of the emission (the 3×3 pixels is approximately equal to the point spread function of the microscope, and may be manually set by the user of the software) as a function of frame number (time). The local background signal is found from the pixels surrounding the QD in each frame and subtracted. If another QD is too close that the local background cannot be determined, then this QD is ignored. Due to the low QD concentration, this occurs very seldom. This results in a set of traces similar to that shown in Figure 6(b). A threshold is set to 2σ of the background signal. It was previously found that if the signal:noise is strong enough, the actual threshold level used (from 2 – 4σ) does not affect the resulting statistics [10]. Then the durations of times spent in the off state and on state are calculated from all the extracted traces and plotted as a probability histogram (Figure 7, normalized to a total probability of 1).

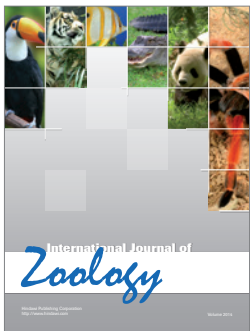
ACKNOWLEDGMENTS

This research is funded by U.S. EPA—Science to Achieve Results (STAR) program, Grant no. R831712, by the National Science and Engineering Research Council of Canada (NSERC) Individual Discovery, Grants no. RGPIN 312970 and RGPIN 250013, as well as NanoInnovation Platform. The authors wish to thank Dr. Andrei Kobitski at the University of Ulm for the Matlab codes used for blinking analysis.

REFERENCES

- [1] J. P. Ryman-Rasmussen, J. E. Riviere, and N. A. Monteiro-Riviere, “Surface coatings determine cytotoxicity and irritation potential of quantum dot nanoparticles in epidermal keratinocytes,” *Journal of Investigative Dermatology*, vol. 127, no. 1, pp. 143–153, 2007.
- [2] R. Hardman, “A toxicologic review of quantum dots: toxicity depends on physicochemical and environmental factors,” *Environmental Health Perspectives*, vol. 114, no. 2, pp. 165–172, 2006.
- [3] J. Lovrić, H. S. Bazzi, Y. Cuie, G. R. Fortin, F. M. Winnik, and D. Maysinger, “Differences in subcellular distribution and toxicity of green and red emitting CdTe quantum dots,” *Journal of Molecular Medicine*, vol. 83, no. 5, pp. 377–385, 2005.
- [4] S. K. Poznyak, N. P. Osipovich, A. Shavel, et al., “Size-dependent electrochemical behavior of thiol-capped CdTe nanocrystals in aqueous solution,” *Journal of Physical Chemistry B*, vol. 109, no. 3, pp. 1094–1100, 2005.
- [5] S. J. Clarke, C. A. Hollmann, Z. Zhang, et al., “Photophysics of dopamine-modified quantum dots and effects on biological systems,” *Nature Materials*, vol. 5, no. 5, pp. 409–417, 2006.
- [6] B. C. Lagerholm, L. Averett, G. E. Weinreb, K. Jacobson, and N. L. Thompson, “Analysis method for measuring submicroscopic distances with blinking quantum dots,” *Biophysical Journal*, vol. 91, no. 8, pp. 3050–3060, 2006.
- [7] M. Nirmal, B. O. Dabbousi, M. G. Bawendi, et al., “Fluorescence intermittency in single cadmium selenide nanocrystals,” *Nature*, vol. 383, no. 6603, pp. 802–804, 1996.
- [8] K. T. Shimizu, R. G. Neuhauser, C. A. Leatherdale, S. A. Emperadoles, W. K. Woo, and M. G. Bawendi, “Blinking statistics in single semiconductor nanocrystal quantum dots,” *Physical Review B*, vol. 63, no. 20, Article ID 205316, 5 pages, 2001.
- [9] A. Y. Kobitski, C. D. Heyes, and G. U. Nienhaus, “Total internal reflection fluorescence microscopy—a powerful tool to study single quantum dots,” *Applied Surface Science*, vol. 234, no. 1–4, pp. 86–92, 2004.
- [10] C. D. Heyes, A. Y. Kobitski, V. V. Breus, and G. U. Nienhaus, “Effect of the shell on the blinking statistics of core-shell quantum dots: a single-particle fluorescence study,” *Physical Review B*, vol. 75, no. 12, Article ID 125431, 8 pages, 2007.
- [11] A. Bachir, N. Durisic, B. Hebert, P. Grüter, and P. W. Wiseman, “Characterization of blinking dynamics in quantum dot ensembles using image correlation spectroscopy,” *Journal of Applied Physics*, vol. 99, no. 6, Article ID 064503, 2006.
- [12] M. Kuno, D. P. Fromm, H. F. Hammann, A. Gallagher, and D. J. Nesbitt, “Nonexponential ‘blinking’ kinetics of single CdSe quantum dots: a universal power law behavior,” *Journal of Chemical Physics*, vol. 112, no. 7, pp. 3117–3120, 2000.
- [13] S. Doose, J. M. Tsay, F. Pinaud, and S. Weiss, “Comparison of photophysical and colloidal properties of biocompatible semiconductor nanocrystals using fluorescence correlation spectroscopy,” *Analytical Chemistry*, vol. 77, no. 7, pp. 2235–2242, 2005.
- [14] R. F. Heuff, J. L. Swift, and D. T. Cramb, “Fluorescence correlation spectroscopy using quantum dots: advances, challenges and opportunities,” *Physical Chemistry Chemical Physics*, vol. 9, no. 16, pp. 1870–1880, 2007.
- [15] U. Banin, M. Bruchez, A. P. Alivisatos, T. Ha, S. Weiss, and D. S. Chemla, “Evidence for a thermal contribution to emission intermittency in single CdSe/CdS core/shell nanocrystals,” *Journal of Chemical Physics*, vol. 110, no. 2, pp. 1195–1201, 1999.
- [16] M. Pelton, D. G. Grier, and P. Guyot-Sionnest, “Characterizing quantum-dot blinking using noise power spectra,” *Applied Physics Letters*, vol. 85, no. 5, pp. 819–821, 2004.
- [17] A. Issac, C. von Borczyskowski, and F. Cichos, “Correlation between photoluminescence intermittency of CdSe quantum dots and self-trapped states in dielectric media,” *Physical Review B*, vol. 71, no. 16, Article ID 161302, 4 pages, 2005.

- [18] M. Kuno, D. P. Fromm, S. T. Johnson, A. Gallagher, and D. J. Nesbitt, “Modeling distributed kinetics in isolated semiconductor quantum dots,” *Physical Review B*, vol. 67, no. 12, Article ID 125304, 15 pages, 2003.
- [19] P. A. Frantsuzov and R. A. Marcus, “Explanation of quantum dot blinking without the long-lived trap hypothesis,” *Physical Review B*, vol. 72, no. 15, Article ID 155321, 10 pages, 2005.
- [20] S. J. Clarke, C. A. Hollmann, F. A. Aldaye, and J. L. Nadeau, “Effect of ligand density on the spectral and affinity characteristics of quantum dot conjugates,” *Bioconjug Chem*, vol. 19, no. 2, pp. 8–562, 2008.
- [21] J. Aldana, Y. A. Wang, and X. Peng, “Photochemical instability of CdSe nanocrystals coated by hydrophilic thiols,” *Journal of the American Chemical Society*, vol. 123, no. 36, pp. 8844–8850, 2001.
- [22] F. Pinaud, D. King, H. P. Moore, and S. Weiss, “Bioactivation and cell targeting of semiconductor CdSe/ZnS nanocrystals with phytochelatin-related peptides,” *Journal of the American Chemical Society*, vol. 126, no. 19, pp. 6115–6123, 2004.
- [23] R. Verberk, A. M. van Oijen, and M. Orrit, “Simple model for the power-law blinking of single semiconductor nanocrystals,” *Physical Review B*, vol. 66, no. 23, Article ID 233202, 4 pages, 2002.
- [24] M. Kuno, D. P. Fromm, H. F. Hamann, A. Gallagher, and D. J. Nesbitt, ““On”/“off” fluorescence intermittency of single semiconductor quantum dots,” *Journal of Chemical Physics*, vol. 115, no. 2, pp. 1028–1040, 2001.
- [25] I. Chung and M. G. Bawendi, “Relationship between single quantum-dot intermittency and fluorescence intensity decays from collections of dots,” *Physical Review B*, vol. 70, no. 16, Article ID 165304, 5 pages, 2004.
- [26] J. A. Kloepfer, R. E. Mielke, M. S. Wong, K. H. Nealson, G. Stucky, and J. L. Nadeau, “Quantum dots as strain- and metabolism-specific microbiological labels,” *Applied and Environmental Microbiology*, vol. 69, no. 7, pp. 4205–4213, 2003.
- [27] J. A. Kloepfer, R. E. Mielke, and J. L. Nadeau, “Uptake of CdSe and CdSe/ZnS quantum dots into bacteria via purine-dependent mechanisms,” *Applied and Environmental Microbiology*, vol. 71, no. 5, pp. 2548–2557, 2005.



Hindawi

Submit your manuscripts at
<http://www.hindawi.com>

